Virus Evolution, 2018, 4(2): vey034

doi: 10.1093/ve/vey034
Research article

Ebola virus, but not Marburg virus, replicates efficiently and without required adaptation in snake cells

Greg Fedewa,[1,†] Sheli R. Radoshitzky,[2,‡] Xiǎolì Chī,[2] Lián Dǒng,[2] Xiankun Zeng,[2,§] Melissa Spear,[3] Nicolas Strauli,[3] Melinda Ng,[4] Kartik Chandran,[4,**] Mark D. Stenglein,[5,††] Ryan D. Hernandez,[6,7,8,9] Peter B. Jahrling,[10,‡‡] Jens H. Kuhn,[10,*,§§] and Joseph L. DeRisi[11,12,*,***]

[1]Integrative Program in Quantitative Biology, Bioinformatics, University of California San Francisco, San Francisco, CA, USA, [2]United States Army Medical Research Institute of Infectious Diseases, Fort Detrick, Frederick, MD, USA, [3]Biomedical Sciences Graduate Program, University of California San Francisco, San Francisco, CA, USA, [4]Department of Microbiology and Immunology, Albert Einstein College of Medicine, Bronx, NY, USA, [5]Department of Microbiology, Immunology, and Pathology, Colorado State University, Fort Collins, CO, USA, [6]Quantitative Biosciences Institute, [7]Institute for Human Genetics, [8]Department of Bioengineering and Therapeutic Sciences, [9]Institute for Computational Health Sciences, University of California San Francisco, San Francisco, CA, USA, [10]Integrated Research Facility at Fort Detrick, National Institute of Allergy and Infectious Diseases, National Institutes of Health, Fort Detrick, Frederick, MD, USA, [11]Department of Biochemistry and Biophysics, University of California San Francisco, San Francisco, CA, USA and [12]Chan Zuckerberg Biohub, San Francisco, CA, USA

*Corresponding authors: E-mail: kuhnjens@mail.nih.gov (J.H.K.); joe@derisilab.ucsf.edu (J.L.D.)

[†]http://orcid.org/0000-0002-3448-3819

[‡]http://orcid.org/0000-0001-8976-8056

[§]http://orcid.org/0000-0003-3526-8755

[**]http://orcid.org/0000-0003-0232-7077

[††]http://orcid.org/0000-0002-0993-813X

[‡‡]http://orcid.org/0000-0002-9775-3724

[§§]http://orcid.org/0000-0002-7800-6045

[***]http://orcid.org/0000-0002-4611-9205

Abstract

Ebola virus (EBOV) disease is a viral hemorrhagic fever with a high case-fatality rate in humans. This disease is caused by four members of the filoviral genus *Ebolavirus*, including EBOV. The natural hosts reservoirs of ebolaviruses remain to be identified. Glycoprotein 2 of reptarenaviruses, known to infect only boa constrictors and pythons, is similar in sequence and structure to ebolaviral glycoprotein 2, suggesting that EBOV may be able to infect reptilian cells. Therefore, we serially passaged EBOV and a distantly related filovirus, Marburg virus (MARV), in boa constrictor JK cells and characterized viral

infection/replication and mutational frequency by confocal imaging and sequencing. We observed that EBOV efficiently infected and replicated in JK cells, but MARV did not. In contrast to most cell lines, EBOV-infected JK cells did not result in an obvious cytopathic effect. Surprisingly, genomic characterization of serial-passaged EBOV in JK cells revealed that genomic adaptation was not required for infection. Deep sequencing coverage (>10,000×) demonstrated the existence of only a single nonsynonymous variant (EBOV glycoprotein precursor pre-GP T544I) of unknown significance within the viral population that exhibited a shift in frequency of at least 10 per cent over six serial passages. In summary, we present the first reptilian cell line that replicates a filovirus at high titers, and for the first time demonstrate a filovirus genus-specific restriction to MARV in a cell line. Our data suggest the possibility that there may be differences between the natural host spectra of ebolaviruses and marburgviruses.

Key words: boa constrictor; diamond python; DpHt cells; ebolavirus; Ebola virus; EBOV; Filoviridae; filovirus; JK cells; marburgvirus; Marburg virus; MARV; virus evolution

Importance

Ebola virus (EBOV) causes severe human disease. The natural host reservoir of EBOV remains unknown. EBOV is distantly related to Marburg virus (MARV), which has been found in wild bats. The glycoprotein of a reptarenavirus known to infect snakes (boas and pythons) is similar in sequence and structure to those of EBOV and MARV. We demonstrate that JK, a boa constrictor cell line, and DpHt, a diamond python heart cell line, do not support MARV infection, but do support EBOV infection without cytotoxicity. These findings suggest that ebolaviruses and marburgviruses may not share identical ecological niches and that filovirus host search efforts may have to be broadened.

1. Introduction

Ebola virus (EBOV) is one of five classified members of the genus *Ebolavirus* in the mononegaviral family *Filoviridae*. Four classified ebolaviruses (Bundibugyo virus, EBOV, Sudan virus, and Taï Forest virus) are known to cause Ebola virus disease (EVD), whereas the fifth classified member, Reston virus (RESTV), is thought to be nonpathogenic for humans. EVD is clinically indistinguishable from Marburg virus disease (MVD), which is caused by the two members of the filoviral genus *Marburgvirus* (Marburg virus [MARV] and Ravn virus [RAVV]) (Kuhn 2018). The largest recorded EVD outbreak, caused by EBOV, began in Western Africa in December 2013 and ended in March 2016, infecting 28,646 and killing 11,323 people (World Health Organization 2016). Like the vast majority of EVD outbreaks (Kuhn 2008; World Health Organization 2016), this outbreak started with a single introduction of EBOV from an unknown wild host reservoir host into a human, with subsequent human-to-human transmission (Baize et al. 2014; Gire et al. 2014; Carroll et al. 2015; Ladner et al. 2015; Park et al. 2015; Simon-Loriere et al. 2015; Tong et al. 2015).

Frugivorous bats are often discussed as potential ebolaviral host reservoirs, but supporting data are overall sparse. These data stem largely from detection of anti-EBOV or anti-RESTV antibodies, short, EBOV genome-like RNA fragments by reverse transcriptase-polymerase chain reaction (RT-PCR), or filovirus-like endogenous viral elements. Ebolaviruses pathogenic for humans have not yet been recovered from any wild bat; complete genomes of pathogenic ebolaviruses have not yet been sequenced from wild bats; and experimental infections of frugivorous bats with ebolaviruses pathogenic for humans have thus far failed (Wahl-Jensen et al. 2013; Jones et al. 2015; Leendertz et al. 2016; Paweska et al. 2016). However, a novel ebolavirus not known to cause disease in any animal, Bombali virus (BOMV), has recently been discovered by next-generation sequencing in oral and anal swabs of Angolan free-tailed bats (*Mops condylurus*) and little free-tailed bats (*Chaerephon pumilus*). This finding indicates that at least some ebolaviruses may infect bats (Goldstein et al. 2018). In contrast, genetically diverse MARV and RAVV, both of which cause human disease, were repeatedly isolated from wild Ugandan Egyptian rousettes (*Rousettus aegyptiacus*) in direct vicinity of human infections (Towner et al. 2009; Amman 2012), and experimental infections of Egyptian rousettes were successful in the laboratory (Jones et al. 2015).

Together, these findings suggest that ebolaviruses and marburgviruses may differ in host tropism. However, few filovirus genus-specific cell susceptibility/permissiveness differences have been uncovered *in vitro*. Notably, African straw-colored fruit bat (*Eidolon helvum*) cells are refractory to EBOV, based on a single amino acid change in the filovirus receptor and binding partner of the EBOV glycoprotein $GP_{1,2}$, Niemann-Pick disease, type C1 protein (NPC1) (Ng et al. 2015). No cell line known to the authors has the opposite differential permissiveness to MARV and EBOV, that is, cell lines permissiveness to ebolavirus infection typically also support marburgvirus infection independent of species origin (Kuhn 2008). Additionally, until now, filoviruses, and specifically EBOV, have only been shown to infect mammalian-derived cell lines.

The recent discovery of a possible evolutionary relationship between the glycoprotein (*GP*) genes of filoviruses and snake-infecting reptarenaviruses (*Arenaviridae*: *Reptarenavirus*) (Gallaher et al. 2001; Amman 2012; Stenglein et al. 2012) prompted us to test the filovirus permissiveness of two snake cell lines. We demonstrate that both boa constrictor JK cells (Stenglein et al. 2012) and diamond python DpHt cells support EBOV replication; that EBOV infection of both cell lines is not accompanied by cytopathic effect (CPE); that JK cells can be infected over multiple passages with EBOV, but not with MARV; and that EBOV does not undergo major genomic adaptation while replicating in JK cells. We also show that MARV restriction occurs at a post-entry stage, most likely during early transcription/replication. Our data support the hypothesis that fundamental differences exist in ebolavirus and marburgvirus host tropism in the wild and indicate a need for further investigation of filovirus host tropism using non-mammalian cell lines.

2. Materials and methods

2.1 Filovirus stock preparation

Infections with Ebola virus/H.sapiens-tc/COD/1995/Kikwit-9510621 (reference genome GenBank #KT582109; EBOV) (Kugelman et al. 2016) and Marburg virus/H.sapiens-tc/KEN/1980/Mt. Elgon-Musoke

(reference genome GenBank #DQ217792; MARV) (Smith et al. 1982) were conducted under biosafety level 4 conditions at the United States Army Medical Research Institute of Infectious Diseases (USAMRIID). EBOV and MARV were propagated in grivet (*Chlorocebus aethiops*) kidney epithelial Vero E6 cells (American Type Culture Collection, Manassas, VA, #CCL-1586) and titrated by plaque assay as described previously (Moe et al. 1981; Shurtleff et al. 2012; Shurtleff et al. 2016).

2.2 Vesiculovirus virus infection assay

Recombinant vesicular stomatitis Indiana viruses (rVSVs) genetically encoding enhanced green fluorescent protein (eGFP) and EBOV or MARV $GP_{1,2}$ protein (rVSV-EBOV $GP_{1,2}$ and rVSV-MARV $GP_{1,2}$, respectively) were previously rescued from cDNAs (Miller et al. 2012; Wong et al. 2010). These viruses were titered on Vero cells (American Type Culture Collection, #CCL-81) as described previously (Wong et al. 2010). Vero cells and boa constrictor (Squamata: Boidae: *Boa constrictor*) kidney JK cells described previously (Stenglein et al. 2012) were plated in respective wells. The next day, cells were infected, and the infection rate was calculated by counting eGFP-positive cells 14–16 h later.

2.3 Filovirus immunostaining

JK, diamond python (Squamata: Pythonidae: *Morelia spilota*) heart (DpHt), or human epithelial adenocarcinoma HeLa cells infected with EBOV or MARV were stained with murine monoclonal antibodies against EBOV or MARV $GP_{1,2}$ (6D8 and 9G4 antibody, respectively), followed by Alexa Fluor 488-conjugated goat anti-mouse IgG (Invitrogen, Thermo Fisher Scientific Waltham, MA, USA) for high-content quantitative image-based analysis. Infected cells were also stained with Hoechst 33342 (blue) and HCS CellMask Red (Invitrogen, Thermo Fisher Scientific) for nuclei and cytoplasm detection, respectively. Infection rates and cell numbers were determined using high-content quantitative imaging data on an Opera quadruple excitation high sensitivity confocal reader (model 3842 and 5025; PerkinElmer, Waltham, MA, USA) at two exposures using ×10 air, ×20 water, or ×40 water objective lenses as described in (Radoshitzky et al. 2010). Analysis of the images was accomplished within the Opera environment using standard Acapella scripts.

2.4 Filovirus virus serial passage

EBOV or MARV were passaged in either JK cells or HeLa cells (American Type Culture Collection #CCL2). For each of the serial passages, JK cells and HeLa cells were plated in six-well plates (at 300,000 cells/well, three replicates per cell line per virus). One day later, cells were exposed to EBOV or MARV at a multiplicity of infection (MOI) of 1. Briefly, exposure was performed by first removing media from cells, incubating cells with media containing filovirus for 1 h, washing cells, and finally adding fresh media back to cells. Infected cells were then incubated at 37°C in a 5 per cent CO_2 atmosphere for 4 or 5 days (Fig. 1). Supernatants were collected at the indicated time points; 50 µl were used to infect monolayers of fresh cells; and 1.5 ml were added to Trizol (Thermo Fischer Scientific) for sequencing.

2.5 Quantification of filoviral titers by qRT-PCR

JK cells were infected with EBOV or MARV (MOI = 1) or mock infected (no virus). At the experimental endpoint, media were harvested for qRT-PCR and/or cells were fixed with formalin (Val Tech Diagnostics, Pittsburgh, PA, USA) prior to immunostaining.

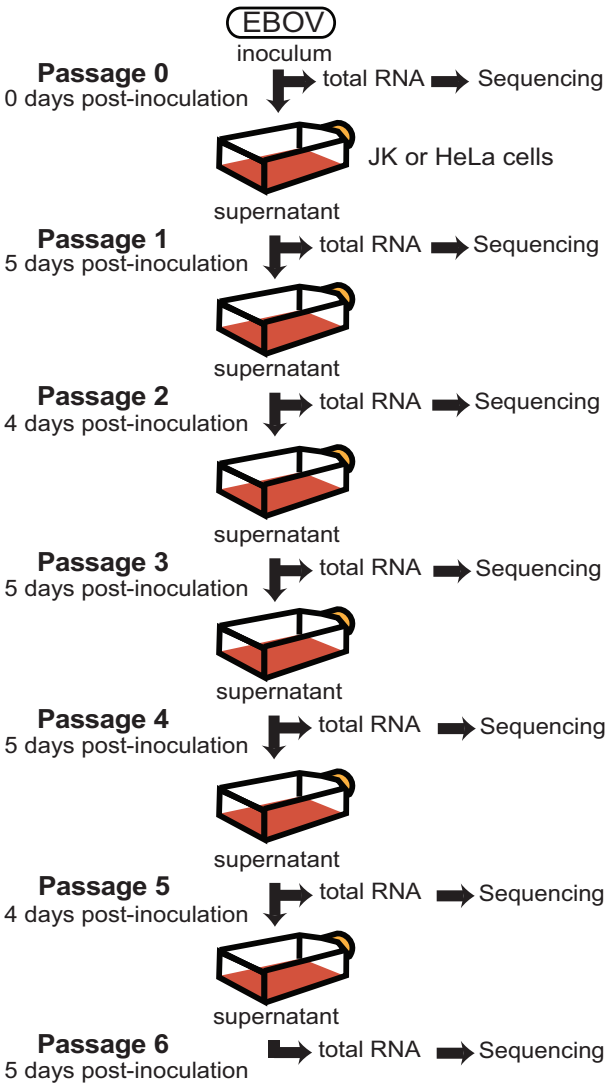

Figure 1. Schematic of the viral passaging experimental procedure. Plated cells, either boa constrictor JK or human HeLa cells, were infected with EBOV for 1 h and then grown for either 4 or 5 days. To passage virus, supernatants were removed and a 1/40 subsample (50 µl) was used to inoculate a fresh monolayer of cells. In addition, 1.5 ml of the supernatant was inactivated for sequencing. This procedure was repeated for a total of six passages of EBOV.

For qRT-PCR, RNA was extracted with Trizol (Thermo Fischer Scientific) and the Ambion Blood RNA Isolation Kit (Thermo Fischer Scientific). The assay was performed with RNA UltraSense one-step kit (Thermo Fisher Scientific) and TaqMan probe (ABI, Thermo Fischer Scientific) following the manufacturer's instructions. The primers used were: EBOGP_For (TGGGCTGAAAACTGCTACAATC), EBOGP_Rev (CTTTGTGCACA TACCGGCAC), probe EBOGP_Prb (5-6FAM-CTACCAGCAGCGC CAGACGG-TAMRA) (Radoshitzky et al. 2010), and MARV_GP2_F (TCACTGAAGGGAACATAGCAGCTAT), MARV_GP2_R (TTGCC GCGAGAAAATCATTT), and probe MARV_GP2_P (ATTGTCAATA AGACAGTGCAC). Serial 10-fold dilutions (10^2 to 10^7) of the assayed virus genomes (RNA) were used as standards.

2.6 Passage population size measurement

The number of EBOV genomes that each cell passage produced and the number of genomes added to sequencing libraries were

determined by two-step reverse transcription droplet digital PCR (RT-ddPCR) (Hindson et al. 2011). EBOV RNA was reverse-transcribed using EBOV-specific primer EBOGP_For (TGGGC TGAAAACTGCTACAATC), diluted, and assayed with the Bio-Rad Qx200 Droplet Digital PCR System (Bio-Rad, Hercules, CA USA) following the manufacturer's instructions.

2.7 Sequencing-library preparations

Trizol-inactivated samples were prepared for Illumina sequencing using a protocol slightly modified from our previously published protocol (Stenglein et al. 2014). Briefly, complementary DNA (cDNA) was created from randomly primed RNA using SuperScript VILO Master Mix (Thermo Fisher Scientific). cDNA was tagmented using Illumina's Nextera reagents (Illumina, San Diego, CA, USA), followed by dual-barcoding to prevent miscalling of samples (Wilson et al. 2016). Libraries were quantified by qPCR, pooled, size-selected using BluePippin (Sage Science, Beverly, MA, USA), amplified, quantified again by qPCR, and paired-end sequenced (150/150 bases) on an Illumina HiSeq 4000 system at the University of California, San Francisco Center for Advanced Technology. Samples HeLa-P1-R1 (Host-Passage-Replicate) and JK-P1-R1 through JK-P6-R1 were prepared and sequenced separately using the same method and sequencer.

2.8 Single nucleotide variant analysis pipeline

Sequencing reads were filtered to remove reads containing sequencing adapters or having a quality below the cut-off of at least 95 per cent of the sequence having a 0.98 probability being correct (-rqf 95 0.98) with PriceSeqFilter from PRICE (version 1.2) (Ruby et al. 2013). Filtered reads were aligned to the EBOV reference genome [GenBank #KT582109 bases 1–18,882] using GSNAP (version 2015-09-29) (Wu and Nacu 2010) with default settings.

Because of the very high coverage in each sample, duplicate reads were not removed, a step usually taken in single nucleotide variant (SNV) analysis. Sorted and indexed BAM files were processed with LoFreq* (version 2.1.2) (Wilm et al. 2012), using default settings, to call SNVs. A final cut-off of $\geq$0.005 allele frequency was selected as a conservative threshold, calculated as 1.25 SDs above the mean of each nucleotide's maximum detected allele frequency (0.00339, $\sigma = 0.00129$) of the Illumina supplied PhiX control sequence, which was included in each sequencing run. SNVs were then determined to be either synonymous or non-synonymous. Analysis was performed and graphs were generated using Python3, IPython (Pérez and Granger 2007), pandas (McKinney 2010), matplotlib (Hunter 2007), and seaborn (Waskom et al. 2016).

2.9 Testing for selection

Briefly, we developed a simulation-based procedure to identify alleles in the EBOV genome that changed frequency over passages more than expected under neutrality given the dynamic viral population size and estimated sequencing error rates (see Supplementary Methods). The neutral simulations had five parameters: the overall population growth function, the number of generations, the starting allele frequency, and the read depth for each site during the first and last passage.

2.10 Detection of defective interfering genomes

Sequencing reads were processed in the same way as for SNV analysis. For each passage point, only properly paired reads were used. All of the passages in JK cells replicate 1 (JK-R1) and the passage HeLa cells replicate 1 passage 1 (HeLa-R1-P1) had a sizable drop in Q-score during sequencing of read 2. These reads were filtered out during pre-processing, necessitating that these paired-end reads be mapped as a combined single-end sample for each of the above passages. These combined samples then lacked proper pairing and were not used in defective interfering (DI) genome analysis. Each of the properly paired reads was also confirmed for the correct mapping orientation. Then the 'reference location' located in each sample's BAM file was used as that read's mapping location, and the distance difference between the read 1 mapping location and read 2 mapping location was calculated along with the mean and SD for the entire set. Proper pairs characterized by a distance difference greater than the mean + 3σ were counted as reads coming from potential DI genomes.

2.11 Measurement of cytopathic effects

Cell numbers were measured as an indication of CPE (see 'Section 2.3 Filovirus immunostaining' for experimental details). Briefly, infected cells were also stained with Hoechst 33342 and HCS CellMask Red for nuclei and cytoplasm detection, respectively. Cell numbers were determined using high-content quantitative imaging data on an Opera quadruple excitation high sensitivity confocal reader.

2.12 Boa constrictor NPC1 sequencing

The boa constrictor NPC1 mRNA sequence was predicted using a draft boa constrictor genome assembly (assembly 'snake_1C') generated as part of the Assemblathon 2 competition (Bradnam et al. 2013). The NPC1 genomic locus is contained on scaffold SNAKE00002789 of the assembly. NPC1 exons were predicted by: (1) comparing to the predicted Burmese python (Squamata: Pythonidae: *Python bivittatus*) NPC1 mRNA (XM_015889305.1); (2) mapping boa constrictor RNA-Seq reads contained in SRA datasets SRR941243 and SRR941236 to the genomic scaffold and to the predicted mRNA/cDNA sequence to validate the predicted exons; (3) comparing the predicted NPC1 protein to other NPC1 protein sequences; and (4) PCR and Sanger sequencing across the predicted sequence, with PCR protocols as described previously (Stenglein et al. 2012). PCR primers used for PCR and Sanger sequencing are listed in Supplementary Table S3.

3. Results

3.1 EBOV and Marburg virus glycoproteins facilitate vesiculovirus infection into snake cells

To test whether snake cells can internalize filoviruses, we first quantified the infection rate of rVSV-EBOV and rVSV-MARV into boa constrictor JK cells and compared it to the infection rate into grivet Vero cells. We used pairwise Welch's *t*-tests to examine if the infection rates were significantly different between the cell lines or between the viruses. For both cell lines, rVSV-MARV generally had a higher rate of infection (Fig. 2). In Vero cells, the difference in infection was significant; the rVSV-MARV titer was 1.035×10^7 infection units (IU) (standard error of the mean [SEM] 2.12×10^6 IU) versus rVSV-EBOV titer of 3.05×10^6 IU (SEM 5.65×10^5 IU) ($P = 0.0171$). In JK cells, the difference was also significant; rVSV-MARV titer was 1.47×10^5 IU (SEM 1.67×10^4 IU) versus the rVSV-EBOV titer of 4.27×10^4 IU (SEM 5.16×10^3 IU) ($P = 0.00106$). In inter-host-type comparisons, JK cells versus Vero cells, JK cells generally had a lower rate of

infection; rVSV-MARV infected JK cells at a very significant infection rate, 1.47×10^5 IU (SEM 1.67×10^4 IU) versus 1.04×10^7 IU (SEM 2.12×10^6) in Vero cells ($P = 0.0048$). rVSV-EBOV infected both cell types at similar rates, 4.27×10^4 IU (SEM 5.16×10^3 IU) in JK cells versus 3.05×10^6 IU (SEM 5.65×10^5 IU) in Vero cells ($P = 0.0031$). Together, these data indicate that both EBOV and MARV glycoproteins bind to and facilitate recombinant vesiculovirus entry into snake cells.

3.2 EBOV, but not Marburg virus, replicates efficiently in snake cells

As the vesiculovirus infection assay indicated that snake JK cells support $GP_{1,2}$-mediated internalization of both rVSV-EBOV and rVSV-MARV, we next tested whether filoviruses can replicate in these cells. We exposed JK cells and diamond python DpHt cells to either EBOV or MARV at MOIs of 1, 5, 10, or no virus (mock). At 72 h after exposure, cells were fixed and stained for filoviral antigen ($GP_{1,2}$) detection (Radoshitzky et al. 2010). Based on immunostaining, both cell lines supported infection of EBOV with dose-dependent infection rates (Fig. 3A). As expected, mock-exposed cells showed little signs of infection; 0.02 per cent ($\sigma = 0.03$) of JK cells were antigen-positive and 0.06 per cent ($\sigma = 0.07$) of DpHt cells were antigen-positive. As the MOI increased to 1, 5, or 10 in JK cells, the number of positive cells increased to 80.64 per cent ($\sigma = 3.74$) (two of the nine wells were not counted for this MOI as they had too few cells), 97.88 per cent ($\sigma = 1.00$), or 99.06 per cent ($\sigma = 0.29$), respectively. Similarly, with the same incremental increases in MOIs, the number of positive DpHt cells increased to 4.10 per cent ($\sigma = 1.75$), 25.28 per cent ($\sigma = 6.36$), or 42.49 per cent ($\sigma = 4.62$), respectively.

Surprisingly, infection rates of cells inoculated with MARV resembled those of mock exposure in both snake cell lines. Based on immunostaining, we measured MARV infection for the mock treatment at 0.24 per cent ($\sigma = 0.18$) for JK cells and 0.02 per cent ($\sigma = 0.02$) for DpHt cells. In JK cells, the number of positive cells increased to 0.24 per cent ($\sigma = 0.07$), 0.82 per cent ($\sigma = 0.59$), or 1.65 per cent ($\sigma = 0.29$) as the MOI increased to 1, 5, or 10, respectively. In DpHt cells, the number of positive cells increased to 0.02 per cent ($\sigma = 0.05$), 0.45 per cent ($\sigma = 0.35$), or 1.84 per cent ($\sigma = 0.82$) as the MOI increased to 1, 5, and 10, respectively. HeLa cells infected with MARV and stained with the same antibody were used as a positive control for the assay and demonstrated its validity (data not shown). Together, these data indicate that snake cells from snakes of at least two diverse species are permissive to EBOV infection but resistant to MARV infection. To our knowledge, JK and DpHt cells represent the first reptilian cell lines permissive to filovirus infection.

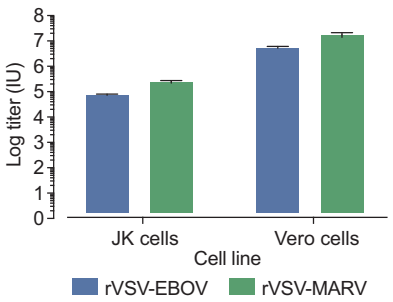

Figure 2. Infection rate of filovirus $GP_{1,2}$-expressing rVSV particles (rVSV-EBOV, rVSV-MARV) on JK cells versus Vero cells. Error bars are equal to the SEM.

3.3 EBOV replicates efficiently in boa constrictor cells over multiple passages

To characterize whether any adaptive genomic mutations are necessary for efficient growth in snake cells, we serially passaged EBOV in JK cells in parallel with control human (HeLa) cells for six cycles (an average of 4.33 days per cycle) (Fig. 1) and MARV, analogously, for five cycles. HeLa cells were chosen as the control because they have been routinely used in filovirus research for both EBOV and MARV (Kuhn 2008). Furthermore, as the viral stocks had been propagated in Vero cells, we could not use Vero cells for virus adaptation studies. The infection of both JK and HeLa cells was initiated at an MOI of 1.

For each passage cycle of EBOV, the extent of infection was monitored by qRT-PCR, immunostaining, and RT-ddPCR. EBOV was detected by qRT-PCR in media from both JK and HeLa cells at all passages. At all passages, EBOV-infected JK cells were characterized by clusters of EBOV $GP_{1,2}$-positive cells, with

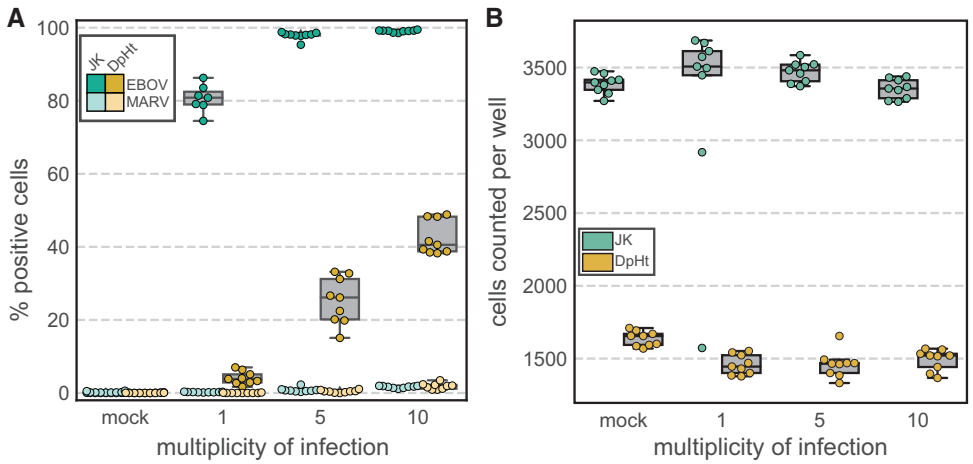

Figure 3. Immunostaining-based filovirus infection rates of snake cell lines. JK cells or DpHt cells were inoculated with EBOV or MARV at MOI of 0 (mock), 1, 5, or 10. At 72 h post-inoculation, supernatant was removed, and cells were fixed. Cells were then stained with Hoechst 33342, HCS CellMask Red, primary antibodies against EBOV or MARV $GP_{1,2}$, and secondary antibodies. The box represents the quartiles and its whiskers extend 150 per cent of the interquartile length. JK cell counts are green, and DpHt cells are dark yellow. EBOV-infected cell counts are depicted in bold; MARV-infected cell counts are in pastel. (A) Percent of cells counted that stained positive for anti-$GP_{1,2}$. (B) Total number of cells counted per well of plated snake cell lines.

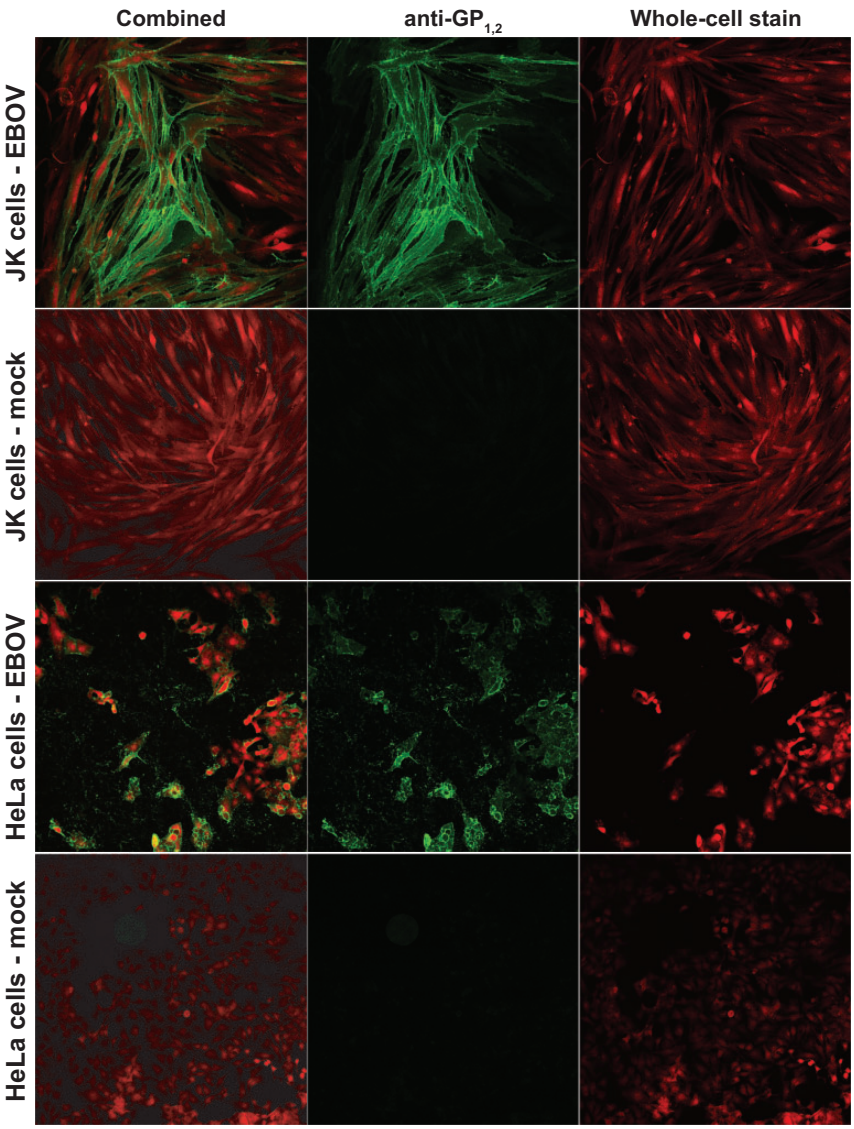

Figure 4. Antibody staining of EBOV $GP_{1,2}$. Cells infected with EBOV were stained with HCS CellMask Red for cytoplasm (shown in red) and for anti-$GP_{1,2}$ antibody (shown in green).

predominantly cytoplasmic and cell membrane staining that was similar to staining in EBOV-infected HeLa cells (Fig. 4). Over the course of these passages, the number of EBOV genome equivalents produced by infected JK cells was modestly lower than that observed with infected HeLa cells. Quantification of EBOV genome copy numbers in the supernatants from passages in JK cells by RT-ddPCR yielded an average of 8.49×10^8 copies/ml ($\sigma = 9.92 \times 10^8$ copies/ml) across all passages and replicates, whereas HeLa cells yielded an average genome copy number of 6.34×10^9 copies/ml ($\sigma = 5.88 \times 10^9$ copies/ml). The EBOV genome copy number measured in the JK supernatants was not significantly different between the first and last passage (4.34×10^9 versus 1.79×10^9 copies/ml, $P = 0.4$, Welch's *t*-test).

For each passage cycle of MARV (projected negative control), the extent of infection was monitored by qRT-PCR. As expected, MARV was detected in the media of all passages in HeLa cells, but only in the media following the first passage in JK cells (Supplementary Table S2).

We used a deep sequencing approach to characterize the spectrum of possible mutations associated with EBOV adaptation to JK cells. For each passage, total cell culture supernatant RNA was processed into cDNA libraries for deep sequencing by random priming. For each library, sequencing reads were aligned to the EBOV reference genome. The mean coverage of the EBOV genome in JK cells across all passages was 36,730-fold ($\sigma = 12{,}016$) and 69,946-fold ($\sigma = 26{,}582$) for HeLa cell passages (Fig. 5). We detected no regional bias of coverage at any point within the genome in any of the three biological replicates of infected JK and HeLa cells, excluding the extreme 5′ and 3′ ends. Previous characterization of cells infected with either EBOV or MARV using deep sequencing yielded a pronounced gradient of filovirus gene transcription similar to that seen for other mononegaviruses. Transcripts accumulate in the 3′ to 5′ direction, with the furthest 3′ gene (encoding the filoviral nucleoprotein [NP]) yielding the highest coverage and the furthest 5′ gene (encoding the filoviral RNA-dependent RNA polymerase [L])

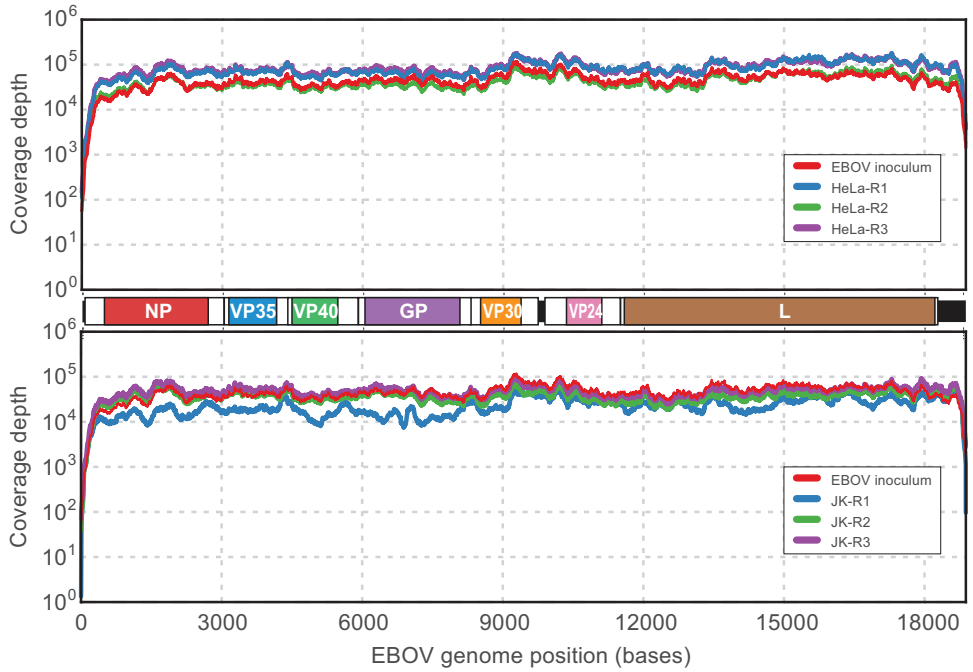

Figure 5. Mean coverage maps of deep sequencing reads mapped to the EBOV reference genome. The EBOV reference genome schematic was drawn to scale between both maps. The number of reads that map to each genome base position was computed for each sample. For each replicate passage series for either HeLa (top graph: EBOV inoculum, red; HeLa-R1, blue; HeLa-R2, green; HeLa-R3, purple) or JK cells (bottom graph: EBOV inoculum, red; JK-R1, blue; JK-R2, green; JK-R3, purple), the mean coverage (respectively colored solid lines) was calculated and graphed.

yielding the lowest coverage (Shabman et al. 2014). For the data presented here, the lack of a 3′ to 5′ coverage gradient is consistent with sequence reads derived from EBOV genomic RNA in cell culture supernatant virions, as opposed to cellular EBOV transcripts (Fig. 5).

In summary, these data identify boa constrictor JK cells as permissive to EBOV, but not to MARV infection. To our knowledge, JK cells represent the first cell line with filovirus genus-specific (ebolavirus versus marburgvirus) permissiveness to EBOV infection.

3.4 EBOV adaption is not required for efficient infection of boa constrictor cells

We first characterized the extent of variation within the EBOV inoculum population. We detected 48 SNVs in the inoculum that passed our quality and frequency cut-off filters including 21 nonsynonymous SNVs (Table 1). We detected only a single position (nt 7,669, EBOV glycoprotein precursor codon 544: T544I) with a nonsynonymous SNV having an allele frequency of >10 per cent in the inoculum (Table 2, Fig. 6A). At this position, the initial population of the inoculum consisted of alleles Thr (62.0%) and Ile (37.9%), similar to the previously characterized EBOV/Kik-9510621 'R4414' (passage 2) strain (Kugelman et al. 2016), and is thought to be an artifact of the previous expansions on Vero cells (Ruedas et al. 2017).

We then characterized variation across passages in JK and HeLa cells. From all replicates and passages, we detected a mean of 89 ($\sigma = 31$) SNVs for passages in HeLa cells and a mean of 51 ($\sigma = 19$) SNVs for passages in JK cells (Table 1, Fig. 7A). Considering only nonsynonymous variants that were not already present in the inoculum, we detected a mean of 15 ($\sigma = 15$) SNVs and 8 ($\sigma = 7$) SNVs for all replicates and all passages in HeLa cells and JK cells, respectively (Table 1, Fig. 7B).

To determine whether a change in the distribution of allele frequencies associated with EBOV SNVs detected was a function of passage or host (boa constrictor versus human) cell, we focused on a comparison of the first and last EBOV passages. The mean allele frequency associated with nonsynonymous SNVs not found in the inoculum for EBOV grown in HeLa cells was 0.009 and 0.015 in in the first passage and passage 6, respectively. The difference between these passages was statistically significant (Kolmogorov–Smirnov [KS] test, $P = 0.00051$; Holm–Bonferroni adjusted $P < 0.01$). However, the difference in distributions of allele frequencies associated with nonsynonymous variants not found in the inoculum for EBOV grown in JK cells was not significant (KS test, $P = 0.41710$; Holm–Bonferroni adjusted $P > 0.01$).

We also compared the distribution of allele frequencies associated with nonsynonymous variants not found in the EBOV inoculum between the two host cells at the last passage. The difference between their means was relatively small (HeLa and JK means of 0.015 and 0.012, respectively), and the difference between these distributions was not statistically significant (KS test, $P = 0.0131$; Holm–Bonferroni adjusted $P > 0.0083$).

To further increase the stringency of our criteria for identifying biologically relevant EBOV variants, we considered only nonsynonymous variants present in all three biological replicates for each passage from each host cell that were not present, or at a frequency below the limit of detection in the inoculum (Table 1, Fig. 7C). We detected a mean of 3 ($\sigma = 2$) nonsynonymous SNVs across all passages in HeLa cells and a mean of 1 ($\sigma = 1$) nonsynonymous SNVs across all passages in JK cells. We were unable to detect any EBOV SNVs that met these criteria for the first passage in either cell type. For JK cell passages, EBOV SNVs that met these criteria were only detected in passages 3, 4, and 6. In passage 6, we did not find any statistical significance between the distributions of allele frequencies of SNVs found in the HeLa cell passage versus the JK cell passage (KS test $P = 0.4249$ versus 0.05).

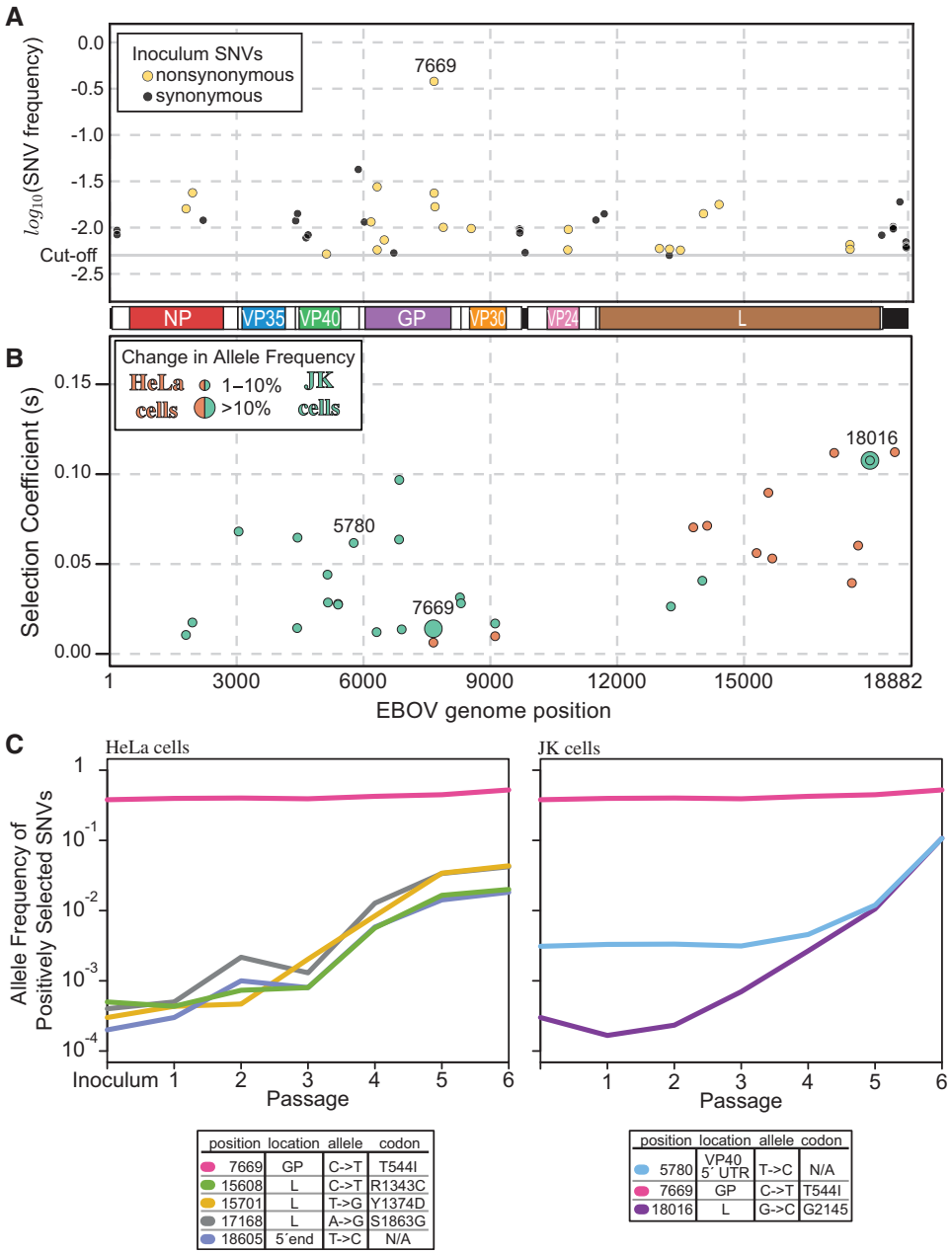

Figure 6. Alleles across the EBOV genome. (A) SNVs found in the EBOV passaging inoculum. The $\log_{10}$ (allele frequency) of each SNV is plotted as a function of its position in the EBOV reference genome (genome schematic drawn to scale between A and B). All SNVs are color-coded. Yellow: non-synonymous SNVs; black: synonymous and non-coding SNVs. (B) The estimated selection coefficients across the EBOV genome for passages in HeLa cells (orange) and JK cells (green). Each point represents the most positively selected allele for each site in the EBOV genome. Selection coefficients were averaged across the three replicates. (C) The allele frequency trajectories across passages of the most strongly selected sites in HeLa (left) and JK (right) cells.

Finally, we implemented a rigorous simulation-based test for neutral evolution of EBOV that takes into account sequencing error, sampling error, and an estimated demographic model representing the passages in our experiments. We found numerous variants that deviate from neutral expectations (14,473 sites in JK and 15,028 sites in HeLa cells). However, as discussed above, nearly all of these variants had extremely small changes in allele frequency. To estimate the strength of selection operating on EBOV in each cell line, we implemented a deterministic fitness model and applied it to each site in turn. We found that the estimated selection coefficients were small (Fig. 6B, and Supplementary Table S1), with only two sites in each set of passages at or above 0.10. In the passages in JK cells, nucleotide 18,016 had an estimated selection coefficient of 0.11 and nucleotide 6,861 had an estimated selection coefficient of 0.10. In the passages in HeLa cells, nucleotides 18,605 and 17,168 both had an estimated selection coefficient of 0.11. These values are on the order of what is seen for selected alleles in humans (results from artificial selection experiments tend to note selection coefficients that are much larger than our results).

Together, these data indicate that EBOV can replicate in boa constrictor cells for prolonged times/passages without requiring major genomic adaptations.

Table 1. Passage of EBOV in HeLa and JK cells.

Host cells	Passage	Replicate	Mean coverage	Total SNVs	Non-syn SNVs	Coding syn SNVs	Non-syn SNVs not in inoculum	Non-syn SNVs in all replicates	Genome copies by RT-ddPCR	Genome copies/ml by RT-ddPCR	Genome copies/ml by RT-qPCR	DI read fraction
Vero E6	0		46,599	48	21	6	N/A	N/A	2.46E+08	4.92E+08	N/A	0.000276
HeLa	1	1	114,414	55	26	5	0	0	N/A	N/A	1.06E+10	N/A
		2	50,683	113	52	19	14		3.11E+10	1.55E+10	1.14E+10	0.000286
		3	114,461	102	46	19	13		3.11E+10	1.55E+10	1.14E+10	0.000344
	2	1	57,860	70	32	9	5	1	3.84E+10	1.92E+10	6.60E+09	0.001306
		2	42273	79	38	12	8		1.69E+10	8.47E+09	4.26E+09	0.001207
		3	110,186	86	36	12	7		2.86E+10	1.43E+10	5.39E+09	0.001629
	3	1	84,746	87	37	12	8	1	2.43E+08	1.22E+08	8.61E+09	0.001437
		2	33,734	54	21	8	2		1.27E+10	6.33E+09	3.49E+10	0.001587
		3	90,833	89	41	10	10		5.39E+09	2.70E+09	2.23E+10	0.001721
	4	1	109,716	80	35	13	10	5	1.97E+08	9.86E+07	1.34E+10	0.000351
		2	51,857	80	38	11	9		8.60E+09	4.30E+09	8.53E+09	0.000364
		3	91,247	80	35	10	7		9.15E+09	4.57E+09	7.36E+09	0.000314
	5	1	79,159	120	60	20	23	5	7.43E+09	3.72E+09	5.12E+09	0.000320
		2	32,086	147	76	37	51		5.59E+09	2.79E+09	5.61E+09	0.000368
		3	65,817	90	43	12	14		9.33E+09	4.66E+09	3.12E+09	0.000365
	6	1	56,325	42	25	7	12	3	1.91E+09	9.56E+08	9.17E+09	0.000512
		2	49,650	165	91	43	61		7.14E+09	3.57E+09	7.73E+09	0.000549
		3	47,332	57	30	7	14		1.89E+09	9.43E+08	6.98E+09	0.000595
JK	1	1	34,972	71	27	8	4	0	1.71E+09	8.53E+08	2.59E+09	N/A
		2	70,411	40	21	4	2		9.31E+09	4.65E+09	2.72E+09	0.000210
		3	103,515	32	15	3	0		2.01E+09	1.01E+09	1.98E+09	0.000157
	2	1	7,237	39	20	6	6	0	7.08E+08	3.54E+08	7.00E+08	N/A
		2	24,005	25	13	1	0		1.25E+09	6.23E+08	3.88E+08	0.000208
		3	24,138	31	13	3	1		4.72E+08	2.36E+08	3.15E+08	0.000209
	3	1	13,131	33	15	3	2	1	5.03E+08	2.52E+08	6.97E+08	N/A
		2	19,078	28	16	3	1		7.68E+08	3.84E+08	8.26E+08	0.000289
		3	20,975	48	22	2	4		1.15E+09	5.76E+08	2.98E+10	0.000255
	4	1	18,038	58	25	9	8	1	1.39E+09	6.95E+08	6.70E+08	N/A
		2	39,866	49	22	8	8		2.50E+09	1.25E+09	6.78E+08	0.000215
		3	66,186	37	19	3	6		1.63E+09	8.15E+08	6.10E+08	0.000225
	5	1	8,475	71	32	18	12	0	3.07E+08	1.54E+08	2.28E+08	N/A
		2	14,266	66	33	13	18		1.22E+09	6.10E+08	2.58E+08	0.000326
		3	16,464	59	29	10	16		2.46E+08	1.23E+08	2.31E+08	0.000307
	6	1	56,183	98	41	24	23	2	1.33E+09	6.66E+08	1.31E+09	N/A
		2	54,147	64	33	9	18		9.81E+08	4.91E+08	6.21E+08	0.000188
		3	60,200	63	31	15	20		3.07E+09	1.54E+09	1.17E+09	0.000225
		Mean	53,521	69	33	11	15/8 (HeLa/JK)		1.27E+10/1.70E+09 (HeLa/JK)			0.00078/0.00023 (HeLa/JK)

syn, synonymous; DI, defective interfering.

3.5 Weak positive selection operates on the EBOV genome during passaging

To identify EBOV genomic sites undergoing positive selection in JK or HeLa cells, we first excluded sites with total read coverage that was not within two SDs of the genome-wide mean (calculated by first averaging the total reads across the three replicates for each passage and then averaging all passages). After filtering, a total of 17,924 sites and 17,970 sites, covering 95 per cent of the genome, were retained for EBOV passaged on HeLa and JK cells, respectively. Only three EBOV genomic sites changed in allele frequency by at least 10 per cent, all of which were identified in JK cell-grown virus (Fig. 7C, Supplementary Table S1): nucleotide positions 5,780 (located in the VP40 5′ untranslated), 7,669 (preGP T544I), and 18,016 (L, a synonymous mutation). In HeLa cells, all allele frequency changes were less than 7 per cent (Supplementary Table S1). Using a deterministic model of positive selection (see Supplementary Methods), we estimated that the selection coefficient at all sites in the EBOV genome (across both HeLa and JK cells) was less than 12 per cent. These data suggest that weak selection can be identified in the EBOV genome over passages (particularly in JK cells; see Supplementary Methods for statistical test results), but that very little adaptation is necessary to successfully passage EBOV in either cell type.

3.6 Passage of EBOV in boa constrictor or hela cells does not lead to major production of defective interfering genomes

The presence of DI particles has been noted with EBOV infection of grivet (*Chlorocebus aethiops*) kidney epithelial Vero E6 cells, but DI

Table 2. EBOV inoculum population sequence variation.

Nucleotide position	Reference allele	SNV allele	SNV %	Gene	Codon change	Sequencing depth
170	C	A	0.93	NP		3,219
172	T	C	0.84	NP		3,217
1805	C	T	1.60	NP	P446S	51,212
1958	C	T	2.38	NP	P497S	60,425
2209	T	C	1.20	NP	S580	29,331
4397	A	G	1.18	VP35		61,244
4441	C	T	1.42	VP40		52,069
4643	C	T	0.78	VP40	A55	30,954
4691	A	G	0.83	VP40	S71	28,166
5125	T	C	0.52	VP40	I216T	28,914
5878	T	G	4.25	VP40		36,349
6023	G	T	1.15	GP		46,354
6179	G	T	1.15	GP	E47D	47,583
6324	G	A	2.75	GP	V96M	49,964
6325	T	C	0.57	GP	V96A	46,789
6493	C	T	0.74	GP	A152V	40,212
6719	C	A	0.53	GP	T227	49,001
7669	C	T	37.95	GP	T544I	36,890
7672	A	C	2.36	GP	E545A	35,520
7692	G	A	1.68	GP	D552N	35,084
7888	A	C	1.01	GP	K617T	35,011
8549	A	G	0.98	VP30	R14G	30,390
9690	A	T	0.97	VP30		73,597
9697	A	C	0.88	VP30		68,562
9698	G	T	0.87	VP30		68,992
9705	A	T	0.93	VP30		63,785
9824	A	G	0.54			67,238
10833	G	A	0.57	VP24	R163K	42,279
10845	T	A	0.95	VP24	L167Q	47,557
11498	G	A	1.21	VP24		43,040
11695	T	C	1.41	L	N38	41,717
13001	A	G	0.59	L	I480V	43,053
13234	A	T	0.50	L	S551	39,465
13240	A	T	0.59	L	K553N	36,367
13497	C	T	0.57	L	A639V	69,958
14043	G	A	1.41	L	R821K	47,806
14412	A	G	1.78	L	E944G	49,799
17507	G	T	0.66	L	D1976Y	46,240
17510	A	C	0.58	L	N1977H	45,945
18259	T	G	0.83	L		41,881
18528	T	C	1.03			28,861
18530	A	T	0.98			29,397
18532	G	A	0.97			29,743
18688	A	G	1.90			34,663
18827	G	C	0.61			39,08
18833	G	T	0.70			3,573
18836	A	C	0.63			3,331
18842	G	C	0.61			3,133

Shown is each of the SNVs found above the cut-off in the inoculum population.

particles remain poorly understood with only a single paper published on EBOV DI genome characterization (Calain et al. 1999). Viral DI particles often contain genomes with long deletions or genomic re-arrangements that presumably arise through errors in replication by, for instance, template switching (Lazzarini et al. 1981). To detect the presence of EBOV genomic sequences with deletions that would likely yield DI particles, we quantified the insertion distance between sequence pairs of EBOV genomes derived from infections of both JK and HeLa cells across all passages and replicates. Distances larger than the library mean + 3σ were counted as being consistent with internal genomic deletions. The EBOV inoculum featured 0.0276 per cent of reads that were consistent with internal genomic deletions. We detected a low level of reads consistent with internal genomic deletion sequences in all passages and replicates on both cell types (mean = 0.0780 per cent (σ = 0.0535) of reads and 0.0234 per cent (σ = 0.00480) of reads for passages on HeLa cells and JK cells, respectively) distributed across the EBOV genome (Table 1, Supplementary Fig. S1). By the final passage, this value changed to 0.0552 per cent (σ = 0.00340) and 0.0206 per cent (σ = 0.00185) of reads for the passage on HeLa and

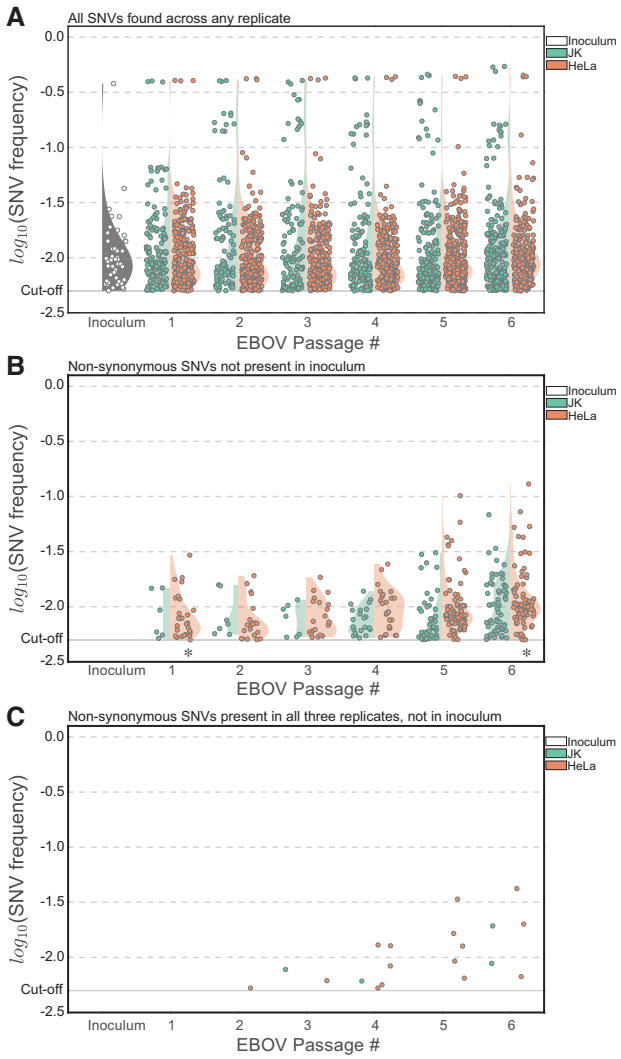

Figure 7. Graphs of EBOV passages versus $\log_{10}$(allele frequency) of single nucleotide variants (SNVs). Each SNV found in each passage was plotted as its $\log_{10}$(allele frequency). (A) Frequency of all SNVs from each replicate. (B) Frequency of nonsynonymous variants from each replicate that were not found in the inoculum. (C) Nonsynonymous variants found in all three replicates, but not the inoculum, were plotted as a single point with their mean frequency. Inoculum was a single replicate, whereas all other passages were pooled triplicates, except for (C). JK cells: green; HeLa cells: orange.

JK cells, respectively. In this analysis, we cannot rule out the possibility of internal deletions produced during sequencing library preparation, and thus these measurements are likely to be overestimates. Regardless, this analysis indicates that sequences consistent with the presence of DI particles could be detected, but only at very low frequencies.

3.7 EBOV does not cause cytopathic effects in snake cells

EBOV $GP_{1,2}$ is thought to be the major cause of the CPE typically seen in EBOV cell culture models (Yang et al. 2000). Typically, $GP_{1,2}$ overexpression results in cell rounding, cell detachment, and cell death. Similar to the method used by Yang et al. (2000) to estimate cytopathic effects of EBOV infection, EBOV-exposed JK cells were stained with Hoechst 33342, imaged, and counted. When compared to mock infection, viable EBOV-infected JK cells did not decrease in number dramatically unlike that observed in many other cell lines (Groseth et al. 2012). At 72 h post-inoculation, we counted a mean of 3,387 (σ = 65) cells/well for wells of mock-infected JK cells and 1,637 (σ = 51) cells/well for wells of mock-infected DpHt cells, whereas EBOV-exposed JK cells were counted at 3,276 (σ = 679) cells/well, 3,471 (σ = 71) cells/well, and 3,353 (σ = 67) cells/well as the MOI increased to 1, 5, or 10, respectively (Fig. 3B). While EBOV-exposed cells at MOIs of 1 and 5 represent statistically significant changes from mock-infected (Welch's *t*-test $P = 0.001$ and $P = 0.018$, respectively), exposure at MOI of 10, which infected a mean of 99 per cent of the cells, showed no significant difference ($P = 0.294$). As the MOI increased to 1, 5, or 10 in EBOV-exposed DpHt cells, cells were counted at 1,458 (σ = 67) cells/well, 1,459 (σ = 90) cells/well, or 1,492 (σ = 72) cells/well, respectively. These values represent statistically significant changes from mock-infected (Welch's *t*-test $P = 0.00001$, $P = 0.0002$, $P = 0.0002$ as the MOI increased to 1, 5, or 10, respectively), but the values are not dose-dependent. Additionally, based on cytoplasmic and nuclear staining of EBOV-infected JK cells, we did not note any obvious morphological changes (Fig. 4).

4. Discussion

The natural reservoir of EBOV and all other ebolaviruses pathogenic for humans remains unclear. Marburgviruses (both MARV and RAVV) were isolated from wild Ugandan Egyptian rousettes (*Rousettus aegyptiacus*) and also were used to infect these bats experimentally (Towner et al. 2009; Amman 2012; Jones et al. 2015). Such findings have not been reported for pathogenic ebolaviruses, thereby raising the possibility that marburgviruses and ebolaviruses may differ in host tropism (e.g., bats of different taxa) and may even infect animals of different orders (Wahl-Jensen et al. 2013; Jones et al. 2015; Jensen Leendertz 2016; Leendertz et al. 2016; Paweska et al. 2016). Experimental filovirus inoculations into taxonomically diverse animals to determine host tropism have only rarely been reported. These experiments suggest that all isolated filoviruses can infect and are frequently lethal for various nonhuman primates (common marmosets [*Callithrix jacchus*], common squirrel monkeys [*Saimiri sciureus*], crab-eating macaques [*Macaca fascicularis*], grivets [*Chlorocebus aethiops*], hamadryas baboons [*Papio hamadryas*], and rhesus monkeys [*Macaca mulatta*]). Most filoviruses can be adapted in the laboratory to infect and kill various rodents (golden hamsters [*Mesocricetus auratus*], guinea pigs [*Cavia porcellus*], laboratory mice), and some filoviruses can infect domestic pigs (*Sus scrofa*). Various plants, goats (*Capra hircus*), horses (*Equus caballus*), and red sheep (*Ovis aries*) were found to be resistant to experimental filovirus infection (summarized in (Swanepoel et al. 1996; Kuhn 2008; Burk et al. 2016)). Interestingly, domestic ferrets (*Mustela putorius furo*) develop disease after experimental infection with various ebolaviruses(Cross et al. 2016; Kozak et al. 2016; Kroeker et al. 2017), whereas MARV or RAVV exposure does not lead to productive infection (Cross et al. 2018; Wong et al. 2018).

In 2001, a possible genetic link between mammalian arenaviruses (family *Arenaviridae*, genus *Mammarenavirus*) and the mononegaviral filoviruses was suggested based on similarities between mammarenaviral GP2 and filoviral GP_2 (Gallaher et al. 2001). This possible link was further substantiated by the structural characterization of GP2 from a newly discovered snake reptarenavirus, CAS virus (genus *Reptarenavirus*), which revealed striking structural similarities to filovirus GP_2 (Koellhoffer et al. 2014). Reptarenaviruses are known to infect captive snakes

(boas and pythons) (Stenglein et al. 2012; Bodewes et al. 2013; Hepojoki et al. 2015; Stenglein et al. 2015), whereas filoviruses infections have not been associated with reptiles. In fact, the thus-far tested reptilian cell lines (e.g., iguana IgH-2, rattlesnake 8625, common box turtle Th-1, Russell's viper VH 2, VSW cells) proved resistant to EBOV infection (van der Groen et al. 1978; Ndungo et al. 2016). Filoviral $GP_{1,2}$s engage endosomal mammalian Niemann-Pick disease, type C1 protein (NPC1) to gain entry into host cells (Côte et al. 2011; Wahl-Jensen et al. 2013). Previously published cell-culture experiments have shown that a single amino acid (Y503), when changed to the analogous human residue (Y503F), causes VH-2 cells to become permissive to EBOV infection (Ndungo et al. 2016).

Whether boa constrictor NPC1 would allow filovirus entry into host cells was not known because although the boa constrictor genome has been assembled, it has not been annotated (Bradnam et al. 2013). We used a comparative alignment approach and mapping of transcriptome-derived short sequence reads to predict the boa constrictor NPC1 protein sequence (Genbank KY595070). The predicted sequence has a Phe residue at the critical position (F517, homologous to F503 in human NPC1), which suggested that boa constrictor cells could be permissive to EBOV infection. Snakes of some species may have been subject to selection by viruses with filovirus-like glycoproteins (Ndungo et al. 2016).

To experimentally test whether snake cells actually support filovirus replication, we exposed boa constrictor JK cells and diamond python DpHt cells to EBOV and MARV. While MARV infection was not productive in these cells, both JK and DpHt cells supported EBOV infection. EBOV infection of JK cells occurred in the absence of CPE, an observation that has been reported only rarely (van der Groen et al. 1978). In addition, JK cells supported EBOV replication over six passages in the absence of major genomic adaptation. Only one genomic position, 7,669, (EBOV preGP T544I) switched major alleles (38%–52%). After maturation of the glycoprotein precursor (preGP), this residue resides in the preGP cleavage product GP_2. The residue is a critical structural determinant of the EBOV GP_2 fusion loop, which mediates fusion of the filovirion membrane with the host-cell membrane to initiate virion entry (Gregory et al. 2014) but could represent a previously identified filovirus cell-culturing artifact (Ruedas et al. 2017).

Both alleles, Thr and Ile, are found in different EBOV isolate sequences. For instance, unpassaged isolates of the EBOV Makona variant (Kuhn et al. 2014b), which caused the 2013–2016 Western African EVD outbreak, almost exclusively encode Thr at pre-GP position 544 (Baize et al. 2014; Gire et al. 2014; Carroll et al. 2015; Ladner et al. 2015; Park et al. 2015; Simon-Loriere et al. 2015; Tong et al. 2015), whereas the passaged 1976 EBOV Yambuku variant isolate encodes the Ile allele (Kuhn et al. 2014a). Likewise, Ile is also encoded at the homologous position in the genome of passaged RESTV (Ikegami et al. 2001; Groseth et al. 2002), which has not yet been associated with human infections. We detected weak positive selection favoring the Ile allele in the EBOV passages in JK cells, suggesting this allele provides a fitness advantage over Thr for infection in JK cells. However, the mechanistic reason for this selection remains to be determined.

In contrast to the successful infections of both rVSV-EBOV and rVSV-MARV, JK cells only supported infection with EBOV. JK cells were unable to support productive MARV infection as demonstrated by the qPCR on viral passaging samples. Taken together, EBOV and MARV are markedly different in their abilities to infect snake cells. Our results suggest that the lack of productive MARV infection in snake cells may be due to a block in the viral lifecycle downstream of virion internalization. Uncovering the molecular underpinnings of this apparent filovirus genus-specific (*Ebolavirus* versus *Marburgvirus*) difference could increase our understanding of filovirus tropism.

Importantly, we do not suggest here that snakes are natural host reservoirs of ebolaviruses (although we also do not rule out this possibility). The cells examined in this study originate from snakes that occur exclusively in South America (boa constrictors) or Australia (diamond pythons)—geographic areas in which filoviruses have not been found thus far. Cell lines from snakes living in Africa or *in vivo* infections of African snakes with filoviruses would have to be performed to even establish a host reservoir hypothesis. Furthermore, filovirus cell tropism *in vitro* does not necessarily predict *in vivo* tropism. For instance, Egyptian rousette cell lines are readily infectable with both marburgviruses and ebolaviruses, but Egyptian rousettes can only be naturally and experimentally infected with marburgviruses and not with ebolaviruses. Our positive EBOV infection results in boa constrictor JK cells, therefore, does not automatically support the idea that boa constrictors could be infected with EBOV. Together, however, our observations raise the possibility that ebolaviruses and marburgviruses could infect evolutionary disparate hosts, possibly even of different animal orders (e.g., mammals versus other classes). Our results suggest that additional nonmammalian cell lines should be screened for filovirus permissiveness to widen or narrow the search for natural filovirus hosts, followed by experimental animal exposures for validation of in vitro results.

Acknowledgements

We thank Laura Bollinger (NIH/NIAID Integrated Research Facility at Fort Detrick, Frederick, MD, USA) for critically editing the article.

Funding

This work was supported by the Chan Zuckerberg Biohub, the Howard Hughes Medical Institute, and in part through Battelle Memorial Institute's prime contract with the US National Institute of Allergy and Infectious Diseases (NIAID) under Contract No. HHSN272200700016I (J.H.K.), and by the US National Human Genome Research Institute (R01 HG007644) to R.D.H.

Data availability

The boa constrictor NPC1 protein sequence was deposited in GenBank under accession KY595070. Raw reads were submitted to the NCBI's Short Read Archive (SRA) under the project ID PRJNA344863.

Supplementary Data

Supplementary data are available at *Virus Evolution* online.

Conflict of interest: None declared.

Disclaimer

The views and conclusions contained in this document are those of the authors and should not be interpreted as necessarily representing the official policies, either expressed or implied, of the US Department of the Army, the US Department of Defense, the US Department of Health and Human Services, or of the institutions and companies affiliated with the authors.

References

Amman, B. R. (2012) 'Seasonal Pulses of Marburg Virus Circulation in Juvenile *Rousettus aegyptiacus* Bats Coincide with Periods of Increased Risk of Human Infection', *PLoS Pathogens*, 8, e1002877.

Baize, S. et al. (2014) 'Emergence of Zaire Ebola Virus Disease in Guinea', *The New England Journal of Medicine*, 371: 1418–25.

Bodewes, R. et al. (2013) 'Detection of Novel Divergent Arenaviruses in Boid Snakes with Inclusion Body Disease in The Netherlands', *The Journal of General Virology*, 94: 1206–10.

Bradnam, K. R. et al. (2013) 'Assemblathon 2: Evaluating *de Novo* Methods of Genome Assembly in Three Vertebrate Species', *GigaScience*, 2: 10.

Burk, R. et al. (2016) 'Neglected Filoviruses', *FEMS Microbiology Reviews*, 40: 494–519.

Calain, P., Monroe, M. C., and Nichol, S. T. (1999) 'Ebola Virus Defective Interfering Particles and Persistent Infection', *Virology*, 262: 114–28.

Carroll, M. W. et al. (2015) 'Temporal and Spatial Analysis of the 2014–2015 Ebola Virus Outbreak in West Africa', *Nature*, 524: 97–101.

Côte, M. et al. (2011) 'Small Molecule Inhibitors Reveal Niemann-Pick C1 Is Essential for Ebola Virus Infection', *Nature*, 477: 344–8.

Cross, R. W. et al. (2016) 'The Domestic Ferret (*Mustela putorius furo*) as a Lethal Infection Model for 3 Species of Ebolavirus', *The Journal of Infectious Diseases*, 214: 565–9.

—— et al. (2018) 'Marburg and Ravn Viruses Fail to Cause Disease in the Domestic Ferret (Mustela putorius furo)', *The Journal of Infectious Diseases*, doi: 10.1093/infdis/jiy268.

Gallaher, W. R., DiSimone, C., and Buchmeier, M. J. (2001) 'The Viral Transmembrane Superfamily: Possible Divergence of Arenavirus and Filovirus Glycoproteins from a Common RNA Virus Ancestor', *BMC Microbiol*, 1: 1

Gire, S. K. et al. (2014) 'Genomic Surveillance Elucidates Ebola Virus Origin and Transmission during the 2014 Outbreak', *Science*, 345: 1369–72.

Goldstein, T. et al. (2018) 'The Discovery of Bombali Virus Adds Further Support for Bats as Hosts of Ebolaviruses', *Nature Microbiology*, doi: 10.1038/s41564-018-0227-2.

Gregory, S. M. et al. (2014) 'Ebolavirus Entry Requires a Compact Hydrophobic Fist at the Tip of the Fusion Loop', *Archives of Virology*, 88: 6636–49.

Groseth, A. et al. (2002) 'Molecular Characterization of an Isolate from the 1989/90 Epizootic of Ebola Virus Reston among Macaques Imported into the United States', *Virus Research*, 87: 155–63.

—— et al. (2012) 'The Ebola Virus Glycoprotein Contributes to but Is Not Sufficient for Virulence *in Vivo*', *PLoS Pathogens*, 8: e1002847.

Hepojoki, J. et al. (2015) 'Arenavirus Coinfections Are Common in Snakes with Boid Inclusion Body Disease', *Journal of Virology*, 89: 8657–60.

Hindson, B. J. et al. (2011) 'High-Throughput Droplet Digital PCR System for Absolute Quantitation of DNA Copy Number', *Analytical Chemistry*, 83: 8604–10.

Hunter, J. D. (2007) 'Matplotlib: A 2D Graphics Environment', *Computing in Science & Engineering*, 9: 90–5.

Ikegami, T. et al. (2001) 'Genome Structure of Ebola Virus Subtype Reston: Differences among Ebola Subtypes', *Archives of Virology*, 146: 2021–7.

Leendertz, S. (2016) 'Testing New Hypotheses regarding Ebolavirus Reservoirs', *Viruses*, 8: 30.

Jones, M. et al. (2015) 'Experimental Inoculation of Egyptian Rousette Bats (*Rousettus aegyptiacus*) with Viruses of the *Ebolavirus* and *Marburgvirus* Genera', *Viruses*, 7: 3420–42.

Koellhoffer, J. F. et al. (2014) 'Structural Characterization of the Glycoprotein GP2 Core Domain from the *CAS Virus*, a Novel Arenavirus-like Species', *Journal of Molecular Biology*, 426: 1452–68.

Kozak, R. et al. (2016) 'Ferrets Infected with Bundibugyo Virus or Ebola Virus Recapitulate Important Aspects of Human Filovirus Disease', *Journal of Virology*, 90: 9209–23.

Kroeker, A. et al. (2017) 'Characterization of Sudan Ebolavirus Infection in Ferrets', *Oncotarget*, 8: 46262–72.

Kugelman, J. R. et al. (2016) 'Informing the Historical Record of Experimental Nonhuman Primate Infections with Ebola Virus: Genomic Characterization of USAMRIID Ebola Virus/H.sapiens-tc/COD/1995/Kikwit-9510621 Challenge Stock "R4368" and Its Replacement "R4415" ', *PLoS One*, 11: e0150919.

Kuhn, J. H. et al. (2014a) 'Reidentification of Ebola Virus E718 and ME as Ebola Virus/H.sapiens-tc/COD/1976/Yambuku-Ecran', *Genome Announcements*, 2: e01178–14.

—— et al. (2014) 'Nomenclature- and Database-Compatible Names for the Two Ebola Virus Variants That Emerged in Guinea and the Democratic Republic of the Congo in 2014', *Viruses*, 6: 4760–99.

—— (2008), *Filoviruses. A Compendium of 40 Years of Epidemiological, Clinical, and Laboratory Studies. Archives of Virology Supplementum*, vol. 20. Vienna, Austria: Springer WienNewYork.

—— (2018), 'Ebolavirus and Marburgvirus Infections', in Jameson J. Larry. et al. (eds.) *Harrison's Principles of Internal Medicine*, 20th edn., vol. 2, pp. 1509–15. Columbus, OH: McGraw-Hill Education.

Ladner, J. T. et al. (2015) 'Evolution and Spread of Ebola Virus in Liberia, 2014-2015', *Cell Host & Microbe*, 18: 659–69.

Lazzarini, R. A., Keene, J. D., and Schubert, M. (1981) 'The Origins of Defective Interfering Particles of the Negative-Strand RNA Viruses', *Cell*, 26: 145–54.

Leendertz, S. A. J. et al. (2016) 'Assessing the Evidence Supporting Fruit Bats as the Primary Reservoirs for Ebola Viruses', *Ecohealth*, 13: 18–25.

McKinney, W. (2010) 'Data Structures for Statistical Computing in Python'. in Proceedings of the 9th Python in Science Conference, pp. 51–56.

Miller, E. H. et al. (2012) 'Ebola Virus Entry Requires the Host-Programmed Recognition of an Intracellular Receptor', *The EMBO Journal*, 31: 1947–60.

Moe, J. B., Lambert, R. D., and Lupton, H. W. (1981) 'Plaque Assay for Ebola Virus', *Journal of Clinical Microbiology*, 13: 791–3.

Ndungo, E. et al. (2016) 'A Single Residue in Ebola Virus Receptor NPC1 Influences Cellular Host Range in Reptiles', *mSphere*, 1: e00007–16.

Ng, M. et al. (2015) 'Filovirus Receptor NPC1 Contributes to Species-Specific Patterns of Ebolavirus Susceptibility in Bats', *Elife*, 4: e11785.

Park, D. J. et al. (2015) 'Ebola Virus Epidemiology, Transmission, and Evolution during Seven Months in Sierra Leone', *Cell*, 161: 1516–26.

Paweska, J. T. et al. (2016) 'Experimental Inoculation of Egyptian Fruit Bats (*Rousettus aegyptiacus*) with Ebola Virus', *Viruses*, 8: 29.

Pérez, F., and Granger, B. E. (2007) 'IPython: A System for Interactive Scientific Computing', *Computing in Science & Engineering*, 9: 21–9.

Radoshitzky, S. R. et al. (2010) 'Infectious Lassa Virus, but Not Filoviruses, Is Restricted by BST-2/Tetherin', *Journal of Virology*, 84: 10569–80.

Ruby, J. G., Bellare, P., and Derisi, J. L. (2013) 'PRICE: Software for the Targeted Assembly of Components of (Meta) Genomic Sequence Data', *G3 (Bethesda, Md.)*), 3: 865–80.

Ruedas, J. B. et al. (2017) 'Spontaneous Mutation at Amino Acid 544 of the Ebola Virus Glycoprotein Potentiates Virus Entry and Selection in Tissue Culture', *Journal of Virology*, 91:

Shabman, R. S. et al. (2014) 'Deep Sequencing Identifies Noncanonical Editing of Ebola and Marburg Virus RNAs in Infected Cells', *MBio*, 5: e02011.

Shurtleff, A. C. et al. (2016) 'Validation of the Filovirus Plaque Assay for Use in Preclinical Studies', *Viruses*, 8: 113.

—— et al. (2012) 'Standardization of the Filovirus Plaque Assay for Use in Preclinical Studies', *Viruses*, 4: 3511–30.

Simon-Loriere, E. et al. (2015) 'Distinct Lineages of Ebola Virus in Guinea during the 2014 West African Epidemic', *Nature*, 524: 102–4.

Smith, D. H. et al. (1982) 'Marburg-Virus Disease in Kenya', *Lancet*, 319: 816–20.

Stenglein, M. D. et al. (2012) 'Identification, Characterization, and *in Vitro* Culture of Highly Divergent Arenaviruses from Boa Constrictors and Annulated Tree Boas: Candidate Etiological Agents for Snake Inclusion Body Disease', *MBio*, 3: e00180–12.

—— et al. (2014) 'Ball Python Nidovirus: A Candidate Etiologic Agent for Severe Respiratory Disease in *Python regius*', *MBio*, 5: e01484–14.

—— et al. (2015) 'Widespread Recombination, Reassortment, and Transmission of Unbalanced Compound Viral Genotypes in Natural Arenavirus Infections', *PLoS Pathogens*, 11: e1004900.

Swanepoel, R. et al. (1996) 'Experimental Inoculation of Plants and Animals with Ebola Virus', *Emerging Infectious Diseases*, 2: 321–5.

Tong, Y.-G. et al. (2015) 'Genetic Diversity and Evolutionary Dynamics of Ebola Virus in Sierra Leone', *Nature*, 524: 93–6.

Towner, J. S. et al. (2009) 'Isolation of Genetically Diverse Marburg Viruses from Egyptian Fruit Bats', *PLoS Pathogens*, 5: e1000536.

van der Groen, G. et al. (1978), 'Growth of Lassa and Ebola Viruses in Different Cell Lines', in S. R. Pattyn (ed.), *Ebola Virus Haemorrhagic Fever* (Amsterdam, The Netherlands: Elsevier/North-Holland Biomedical Press), 255-60.

Wahl-Jensen, V. et al. (2013), 'Role of Rodents and Bats in Human Viral Hemorrhagic Fevers', in Sunit K. Singh and Daniel Ruzek (eds.), *Viral Hemorrhagic Fevers*, 99–127. Boca Raton, FL: Taylor & Francis/CRC Press.

Waskom, M. et al. (2016) 'seaborn: v0.7.0 (January 2016)', *zenodo* http://doi.org/10.5281/zenodo.45133.

Wilm, A. et al. (2012) 'LoFreq: A Sequence-Quality Aware, Ultra-Sensitive Variant Caller for Uncovering Cell-Population Heterogeneity from High-Throughput Sequencing Datasets', *Nucleic Acids Research*, 40: 11189–201.

Wilson, M. R. et al. (2016) 'Multiplexed Metagenomic Deep Sequencing to Analyze the Composition of High-Priority Pathogen Reagents', *mSystems*, 1: e00058–16.

Wong, A. C. et al. (2010) 'A Forward Genetic Strategy Reveals Destabilizing Mutations in the Ebolavirus Glycoprotein That Alter Its Protease Dependence during Cell Entry', *Journal of Virology*, 84: 163–75.

Wong, G. et al. (2018) 'Marburg and Ravn Virus Infections Do Not Cause Observable Disease in Ferrets', *Journal of Infectious Diseases*, doi: 10.1093/infdis/jiy245.

World Health Organization (2016), 'Ebola situation reports' <http://apps.who.int/ebola/ebola-situation-reports> accessed 16 Oct 2018.

Wu, T. D., and Nacu, S. (2010) 'Fast and SNP-Tolerant Detection of Complex Variants and Splicing in Short Reads', *Bioinformatics*, 26: 873–81.

Yang, Z.-Y. et al. (2000) 'Identification of the Ebola Virus Glycoprotein as the Main Viral Determinant of Vascular Cell Cytotoxicity and Injury', *Nature Medicine*, 6: 886–9.